

Optimal Quantum Control of Charging Quantum Batteries

R. R. Rodríguez,¹ B. Ahmadi,¹ G. Suárez,¹ P. Mazurek,¹ S. Barzanjeh,² and P. Horodecki¹

¹*International Centre for Theory of Quantum Technologies,
University of Gdansk, Jana Bażyńskiego 1A, 80-309 Gdansk, Poland*

²*Department of Physics and Astronomy, University of Calgary, Calgary, AB T2N 1N4 Canada*

Quantum control allows to address the problem of engineering quantum dynamics for special purposes. While recently the field of quantum batteries has attracted much attention, optimization of their charging has not benefited from the quantum control methods. Here we fill this gap by using an optimization method. We apply for the first time this convergent iterative method for the control of population of a bipartite quantum system for two cases. First, we apply it for a qubit-qubit case. The quantum charger-battery system is considered where the energy is pumped into the charger by an external classical electromagnetic field. Second we systematically develop the original formulation of the method for two harmonic-oscillators in the Gaussian regime. In both cases the charger is considered to be an open dissipative system. Our optimization takes into account the experimentally viable problem of turning-on and off of the external laser field. Optimising the shape of the pulse significantly boosts both power and efficiency of the charging process in comparison to the known results. Optimization of charging of harmonic-oscillator batteries is particularly simple, as the optimal pulse found in zero-temperature regime stays so for any arbitrary temperature.

I. INTRODUCTION

Energy processing in quantum systems attracts attention for both fundamental and practical reasons. While second law of thermodynamics holds in its generalised form [1–4], relinquishing classical constraints in microscopic thermal machines may lead to boost in their power [5–7]. Potential for quantum advantage was one of the factors (apart from sheer curiosity) motivating research in microscopic thermal machines, both from the quantum open system [8–12] (see Ref. [13] for a comprehensive review) and resource theory [14–18] perspectives. Proposals of their realisations [19–21] were recently followed by experimental implementations in trapped ion systems [22–24].

Quantum battery [13] is a system which stores useful energy (work), and as such may be integrated into a thermal machine, which operates with the aim of charging the battery. Alternatively, quantum batteries are of independent interest as reservoirs of energy which can be stored and released on demand. Both qubits and harmonic oscillators were considered in this role [25, 26]. Possible application of these systems is to provide energy for operations on low temperature quantum systems from within, as an alternative to energy transfer from exterior sources, leading to noise. In many body systems, collective effects have been shown to enable quantum advantage in charging power [27–30], similarly to metrological settings. Spin chains [31], superconducting qubits and quantum dots [32], disordered chains [33, 34], and qubits in an optical cavity [26] were all investigated from the perspective of their use as quantum batteries.

The open system description of charging of quantum batteries enables to encapsulate noise effects, always present in realistic settings. A quantum battery (typically a qubit or a quantum oscillator) is coupled to an additional quantum system, called charger (see Fig. (1)). It is the charger which interacts with external laser field,

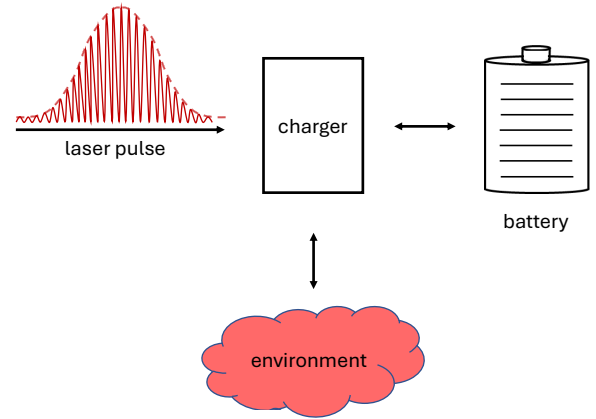


FIG. 1: Battery charging: a quantum system, battery, is coupled to another quantum system, charger. The charger is pumped by classical electromagnetic field while interacting with environment. Goal: taking into account all the couplings, optimize over pulse shape such that the the battery achieves high energy and ergotropy at a given time.

as well as with environment. This arrangement on one hand allows for the flow of energy from the field to the battery, while on the other partially isolates it from the effects of noise, improving quality of stored energy. While quantifiers of this quality may vary for particular physical applications, here we are going to use ergotropy [35]. The general setup for battery charging is described in more detail in Sec. II.

Different methods are used to improve power and quality of charging. An example of a passive method is to exploit qutrit batteries with energy landscape favouring charging through the so-called dark states [36, 37], while measurements [38], empowered by linear feedback proto-

cols [39] have been shown to exhibit improvement with respect to charging which do not take noise into account.

Here, we develop a passive method for charging quantum batteries of an arbitrary dimension through chargers coupled to classical electromagnetic field and memoryless environment. The method relies on an iterative numerical technique [40–42] for optimizing a functional, which in our case encodes the goal state of the battery and the dynamics of the open system, including noise and external driving. We choose the goal state of the battery to be maximally excited (in case of a qubit) or a specific pure state (in case of a harmonic oscillator battery). The result is a time profile of the electromagnetic field which drives the battery state close to the goal state in a desired time. By a design of the functional, we enforce shape pulses of the field to increase smoothly from zero values at the beginning of the protocol (and vanish in the same manner at the end), which addresses the problem of switching on and off of the laser field, and ensures practicality of obtained solutions. Our method works not only for pure, but also mixed states, which enables us to analyze charging for non-zero temperatures of the environment. The method is presented in Sec. III.

When applied to qubit atomic batteries inside an optical cavity (Sec. IV), the method leads to battery states of higher energy and ergotropy than the ones previously reported in Ref. [43] for experimentally viable parameters. Remarkably, while our method is not fully optimized for minimizing the energy cost of charging, it leads to protocols with lesser energy consumption than the ones reported for qubit batteries. Moreover, in Sec. V we show that the same applies to charging of harmonic oscillator batteries with linear coupling, while in this case optimization over temperature is not needed, provided charger and battery are prepared in the vacuum state.

II. GENERAL SETUP

We will investigate the process of charging quantum batteries when both charger and the batteries are either qubits or oscillators. The charger is assumed to dissipate energy into the environment during the charging process. The local GKLS master equation [44] will be used to describe the dissipative evolution of the whole system. The process starts from the charger in the ground state driven by a classical laser field. The goal is to design an optimized laser pulse such that the final state is achieved at a given time. With the aim to demonstrate efficient charging of qubit and oscillator quantum batteries, we select their final states to be excited and some coherent states, respectively.

Quality of the final state is going to be assessed by its ergotropy. Ergotropy is defined as the maximum amount

of work that can be extracted from a state ρ in a cyclic unitary process such that the initial Hamiltonian of the system $H(t_0)$ is equal to the final Hamiltonian of the system $H(t_f)$ [35]. Defining $E(\rho) := \text{tr}\{H\rho\}$ as the internal energy of the system, ergotropy of a state ρ is calculated as

$$\mathcal{E}(\rho) := E(\rho) - E(\rho_p), \quad (1)$$

where ρ_p is the passive state associated with ρ by $\rho_p = \min_U U\rho U^\dagger$, with the minimization over all unitaries. Since the ground state is a passive state only for pure states, in the optimization process we choose the target state of the battery to be an excited pure state to maximize the ergotropy. As a figure of merit we compute the ratio $\frac{\mathcal{E}(\rho)}{E(\rho)}$ for the battery at the final time t_f and show the advantage of the use of the optimized pulse when increasing the temperature of the environment. In Refs. [26, 43, 45–47] quantum correlations and quantum coherence contained in the initial state of the charger were investigated for possible benefits in transferring energy from quantum chargers to quantum batteries. As specific preparations of the initial state of the charger may cost significant input energy, here we relax these requirements while achieving more pronounced energy transfer and ergotropy extraction in the battery.

III. CONVERGENT ITERATIVE METHOD FOR CONTROL OF THE POPULATION OF A QUANTUM SYSTEM

A. Application to battery charging

In order to charge a quantum battery, we desire that our initial state (representing the discharged battery) evolve to a target final state (representing the battery fully charged) under some dynamical evolution in a given time, τ . In this paper, we are only interested in the evolution of open systems, therefore the equation of motion of our system will be given by the Liouvillian operator i.e.

$$\frac{d\hat{\rho}}{dt} = \mathcal{L}\hat{\rho}, \quad \hat{\rho}(t_0) = \hat{\rho}_0, \quad (2)$$

where $\hat{\rho}_0$ is the initial state. The Liouvillian operator takes into account the local Hamiltonians, dissipation terms and the classical drive. Under this evolution constraint, driving the system to the desired final state while limiting the energy spent on the drive can be understood through the problem of minimization of the general functional

$$J[\rho^{(i)}(T), \epsilon^{(i)}(t)] = J_T(\rho^{(i)}(T)) + \int_0^T g_a(\epsilon^{(i)}(t)) dt, \quad (3)$$

where $\rho^{(i)}(T)$ denotes the state at the final time T evolved by the field of iteration i , $\epsilon^{(i)}(t)$. J_T is the main part of the functional J and throughout the paper it corresponds to $J_T = 1 - \mathcal{F}^i(T)$, where $\mathcal{F}^i(T) = \text{tr}[\hat{\rho}^{\text{tgt}\dagger} \hat{\rho}^i(T)]$ is the fidelity between the pure states $\hat{\rho}^i(T)$ and $\hat{\rho}^{\text{tgt}}$. Here, $\hat{\rho}^{\text{tgt}}$ denotes the target state.

As we explain below, the remaining part of the functional attests for the energy cost of the drive:

$$\begin{aligned} g_a(\epsilon^{(i)}(t)) &= \frac{\lambda_a}{S(t)} (\epsilon^{(i)}(t) - \epsilon^{(i-1)}(t))^2 \\ &= \frac{\lambda_a}{S(t)} (\Delta\epsilon^{(i)}(t))^2, \end{aligned} \quad (4)$$

where $\lambda_a > 0$ is a numerical parameter for the optimization and $S(t) \in [0, 1]$ allows for the control of the shape of the pulse. Throughout this work $S(t)$ has the form

$$S(t) = \begin{cases} \sin^2\left(\frac{\pi}{2} \frac{t}{t_{\text{on}}}\right) & \text{for } 0 \leq t \leq t_{\text{on}} \\ 1 & \text{for } t_{\text{on}} < t < \tau - t_{\text{off}} \\ \sin^2\left(\frac{\pi}{2} \frac{(\tau - t)}{t_{\text{off}}}\right) & \text{for } \tau - t_{\text{off}} \leq t \leq \tau, \end{cases} \quad (5)$$

where $t_{\text{on}} = t_{\text{off}} = 0.005\tau$. We take the initial guess for the field in the form $\epsilon^{(i=0)}(t) = S(t)\kappa$. For a specific case, we choose κ large enough to achieve fast convergence. The term (4) quantifies the divergence of the pulse shape at iteration i from the shape in the previous iteration. We select pulse shapes with small energies in the initial iterations, in order to obtain a final pulse shape solutions which is not energetically costly.

The reasoning for the choices of $S(t)$ and $\epsilon^{(i=0)}(t)$ is the following: we start with the field guess $S(t)\kappa$ which has small values at initial and final stages of the evolution. Minimization of the functional with $S(t)$ going to 0 in these limits suppresses substantial modification of values of the field in the initial and final time regimes, compared to modification of the values of the field in intermediate times. The result is that the optimized pulse smoothly achieves small values at initial and final times. Essentially, the optimization strategy is finding a way to ensure that at each iteration the value of the functional diminishes, i.e.

$$J[\rho^{(i+1)}(T), \epsilon^{(i+1)}(T)] \leq J[\rho^{(i)}(T), \epsilon^{(i)}(T)]. \quad (6)$$

Following the original proof of convergence [40] for closed-system dynamics we see that Eq. (6) is satisfied when the update of the field is

$$\Delta\epsilon^{(i)}(t) = \frac{S(t)}{\lambda_a} \text{Im} \left[\text{tr} \left\{ \hat{\sigma}^{(i-1)}(t) \left(\frac{i\partial\mathcal{L}}{\partial\epsilon(t)} \Big|_{(i)} \right) \hat{\rho}^{(i)}(t) \right\} \right]. \quad (7)$$

where ρ and σ represent the density matrix of the forward and backward states respectively. Above, we used a shorthand for

$$\frac{\partial\mathcal{L}}{\partial\epsilon(t)} \Big|_{(i)} = \frac{\partial\mathcal{L}}{\partial\epsilon(t)} \Big|_{\epsilon(t)=\epsilon^{(i)}(t)}. \quad (8)$$

While in general this derivative has to be numerically calculated, this is not the case for charging protocols investigated in this work, where the corresponding Liouvillians are linear in the control field. $\hat{\sigma}^{(i-1)}$ are the so-called backward states and they evolve according to [62]

$$\frac{d\hat{\sigma}}{dt} = -\mathcal{L}^\dagger \hat{\sigma}, \quad \hat{\sigma}(T) = \hat{\rho}^{\text{tgt}}, \quad (9)$$

where the time goes backwards. Having said that, we can proceed to sketch the algorithm. To simplify the explanation, we will consider that $\frac{\partial\mathcal{L}}{\partial\epsilon(t)}$ does not depend on time. We consider a time grid made of $N + 1$ time points with the step between them equal to dt . The grid starts at $t = 0$ and ends at $t = \tau$ and the states are only defined at those points. We use the notation $\epsilon^{(i=1)}(t)$ for the initial guess of the field. First of all, for the time step i we generate $\hat{\sigma}^{(i-1)}(t)$ by propagating the backward states $\hat{\sigma}$ using Eq. (9) with field $\epsilon^{(i)}(t)$ from $t = \tau$ to $t = 0$ along the $N + 1$ time points. Then, we calculate the update of the field with our initial state $\hat{\rho}_0$ using the discretized version of Eq. (7) as

$$\Delta\epsilon^{(i)}(\bar{t}) = \frac{S(\bar{t})}{\lambda_a} \text{Im} \left[\text{tr} \left\{ \hat{\sigma}^{(i-1)}(t) \left(\frac{i\partial\mathcal{L}}{\partial\epsilon(t)} \Big|_{(i)} \right) \hat{\rho}^{(i)}(t) \right\} \right], \quad (10)$$

where instead of computing the update for time t we will do so for time $\bar{t} = t + dt/2$. Doing so, we can solve the apparent contradiction of Eq. (7) where the update of the field is calculated at time t whereas the states used for the computation are also at time t and to get those, we will need to propagate them under the field we are calculating now. Therefore, calculating it at \bar{t} , the update only depends on the past information. Actually, Eq. (7) is the continuous limit of Eq. (10) when $dt \rightarrow 0$.

With this update, we can propagate our states $\hat{\rho}$ under the new field while at the same time we keep updating the field sequentially for all time grid, obtaining $\hat{\rho}^{(i)}(t)$ and $\epsilon^{(i)}(t)$. In doing this, we extend the field values calculated at points $t + dt/2$ to points $t + dt$, tacitly assuming that discretization of the evolution equations does not lead to rapidly oscillating field (this can always be obtained by decreasing dt). After that, we move to the next step, $i + 1$, where the guess field will correspond to the updated field of the iteration from before. This procedure keeps repeating until the convergence of the functional Eq. (3).

It is worth to emphasize that the convergence is guaranteed only in the case the field is continuous in time.

IV. QUBIT-QUBIT MODEL

We start by considering a system composed of a quantum charger charging a quantum battery made of l cells (l qubits), while a classical laser field $\epsilon(t)$ is shining on the charger. The Hamiltonian of the whole system reads ($\hbar = 1$)

$$H = H_A + H_B + H_{AB} - \mu\epsilon(t)\sigma_A^x \otimes \mathbb{I}_B, \quad (11)$$

where $H_A = \frac{\omega}{2}(-\sigma_A^z + \mathbb{I}_A) \otimes \mathbb{I}_B$ and $H_B = \mathbb{I}_A \otimes \sum_{k=1}^l \omega(-\sigma_k^z + \mathbb{I}_k)/2$ are the free Hamiltonians of the charger and the battery, respectively, and $H_{AB} = \sum_{k=1}^l g(\sigma_A^+ \sigma_{B,k}^- + \sigma_A^- \sigma_{B,k}^+)$ the interaction Hamiltonian in which g is the interaction strength. As we are considering real quantum systems, dissipation is inevitable to occur due to the interaction with the environment. Here, the dissipation is taken into account following the spirit of [43]. We assume that the charger is interacting weakly with the environment such that its dynamics can be described via a Markovian master equation. The master equation of the whole system of the charger plus the battery reads

$$\dot{\rho}_{AB} = -i[H, \rho_{AB}] + \mathcal{D}_T[\rho_{AB}], \quad (12)$$

where H is the Hamiltonian of the whole system defined in Eq. (11) and $\mathcal{D}_T[\cdot]$ the Lindblad super-operator which accounts for the dissipation and is represented by

$$\mathcal{D}_T[\rho_{AB}] = \gamma(N_b(T) + 1)\mathcal{D}_{\sigma^-}[\rho_{AB}] + \gamma N_b(T)\mathcal{D}_{\sigma^+}[\rho_{AB}], \quad (13)$$

where

$$N_b(T) = \frac{1}{\exp[\omega/(K_B T)] - 1}, \quad (14)$$

T is the temperature of the bath, γ fixes the time scale of the dissipation and $\mathcal{D}_b(\cdot) = b(\cdot)b^\dagger - 1/2\{b^\dagger b, \cdot\}$ for any operator b . The initial states of the charger and the battery are assumed to be the ground states. The goal is to design a pulse for the laser field such that the final battery state has maximum ergotropy. To do so, our target state is the excited state of the battery, $|e\rangle$. We will compare our results obtained when optimizing the field appearing in Eq. (11) with the case of using an oscillatory field interacting with the charger modelled by the following Hamiltonian [43]

$$H = H_A + H_B + H_{AB} + F(e^{i\omega t}\sigma_A^+ + e^{-i\omega t}\sigma_A^-) \otimes \mathbb{I}_B, \quad (15)$$

where H_A , H_B and H_{AB} are the same as in Eq. (11). A figure of merit for our comparison is the energy used by the fields in the two different settings (always considering that the coupling constants μ and F are the same (see

Appendix VIII A). We compute this as the integral of the field squared i.e.

$$\mathcal{W}_\tau = \int_0^\tau dt |\epsilon(t)|^2, \quad (16)$$

where τ is the final time of the evolution. For the case of the oscillatory field the energy can be computed as (see Appendix VIII A)

$$\mathcal{W}_{\tau,osc} = 2\tau + \frac{1}{\omega} \sin(2\omega\tau). \quad (17)$$

We compare the energy and ergotropy of the battery in both settings in Fig. 2, where battery in the excited state is the target state. We see that the difference in the values of ergotropy between them is not very noticeable. Nevertheless, the improvement when optimizing the field becomes apparent when looking at the energy spent from the field. For the single qubit case, the energy spent from the optimized field is $\mathcal{W}_{\tau,opt} \approx 6.38$ and from the non-optimized one $\mathcal{W}_{\tau,osc} \approx 31.42$. For the case of 3 cells, we still get an improvement in the results even though the advantage in the energy used by the field is not as big as before, being the energy spent by the field $\mathcal{W}_{\tau,opt} \approx 27.61$ compared to $\mathcal{W}_{\tau,osc} \approx 31.42$.

In Fig. 3a ergotropy extraction of the battery and energy used by the optimized field at time $t = \frac{\pi}{g}$ for different temperatures are plotted. As is observed due to the increase of noise the ergotropy extractions for the optimized field approaches that of the oscillatory field and at last both go to zero.

In Fig. 3b the energy used by the field first is plotted for different temperatures of the bath. We can distinguish three different trends. First of all, energy decreases from temperature 0 to some non-zero value ($N_b(T) \approx 1$) and this can be explained as the environment feeding energy to the system -due to the terms of the dissipator that go with $N_b(T)$ -. The second trend corresponds to the increasing of energy spent when increasing the average number of photons of the bath $N_b(T)$. This can be explained by the fact that when increasing the temperature, the bath injects more noise into the system and it is more difficult for the optimization to get good ratios between ergotropy and energy. Finally, as we keep increasing the temperature, it becomes impossible for the optimized external field to make the system evolve to the target state because the system quickly thermalizes to the Gibbs state with zero ergotropy and the optimization does not ask for energy from the optimized field.

We note that in principle a more careful optimization over initial conditions may give one better results than those presented here.

V. OSCILLATOR-OSCILLATOR MODEL

Finally we investigate the case in which both the charger and the battery are harmonic oscillators and the

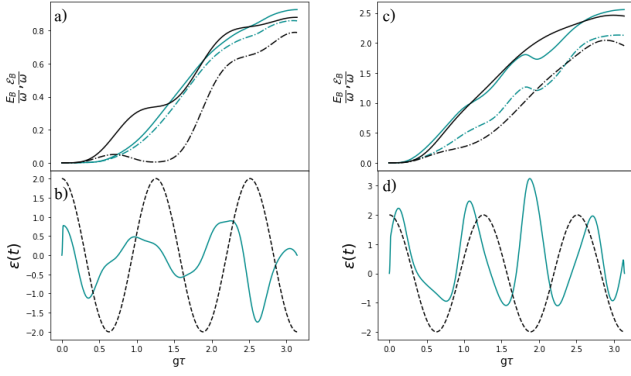


FIG. 2: Single qubit battery (a), (b) vs 3 qubit battery cells (c), (d) at zero temperature $N_b(T) = 0$, with coupling constants $g = 0.2\omega$, $\gamma = 0.05\omega$, $F = \mu = 0.5\omega$. In (a,b) the amplitude of the guess field is $\kappa = 0.5$ and for (c,d) $\kappa = 0.75$. (a,c) Energy (dashed line) and ergotropy (dotted line) versus $g\tau$ in the case of optimizing the field (in green) and in the case of using an oscillatory field (in black). The final time is chosen such that the energy and ergotropy extraction achieve their maximum value for the oscillatory field. The target state is the excited state for the battery. (b,d) The corresponding field pulses.

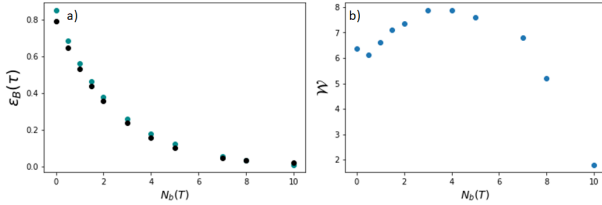


FIG. 3: (a) Ergotropy extraction of a single qubit battery at time $t = \frac{\pi}{g}$ for different temperatures of the environment, with coupling constants $g = 0.2\omega$, $\gamma = 0.05\omega$, $F = \mu = 0.5\omega$ and the amplitude of the guess field $\kappa = 0.5$. As it is seen due to the increase of noise the ergotropy extractions for the optimized field (cyan) approaches that of the oscillatory field (black) and at last go to zero. (b) Energy consumed by the field for different temperatures of the environment. Energy spent by the oscillatory field is 31.42 for all temperatures. The same parameters as in (a). Similar plots are obtained for 3 qubit case.

charger suffers from dissipation. The Hamiltonian of our model reads

$$H = H_A + H_B + H_{AB} - \mu\epsilon(t)(a + a^\dagger) \otimes \mathbb{I}_B, \quad (18)$$

where $H_A = \omega a^\dagger a \otimes \mathbb{I}_B$ and $H_B = \mathbb{I}_A \otimes \omega b^\dagger b$ are the free Hamiltonians of the charger and the battery, respectively, and the interaction Hamiltonian reads $H_{AB} = g(ab^\dagger + a^\dagger b)$. In addition, the charger interacts weakly with the bath. Consequently, the dynamics is described by the Lindblad master Eq. (12), with the Lindblad super-operator accounting for dissipation expressed by

$$\mathcal{D}_T[\rho_{AB}] = \gamma(N_b(T) + 1)\mathcal{D}_a[\rho_{AB}] + \gamma N_b(T)\mathcal{D}_{a^\dagger}[\rho_{AB}], \quad (19)$$

where $\mathcal{D}_c(\cdot) = c(\cdot)c^\dagger - 1/2\{c^\dagger c, \cdot\}$ for any operator c . The total Hamiltonian H is quadratic, and consequently the evolution preserves the Gaussian character of the initial state. For the initial Gaussian state taken to be the ground state of harmonic oscillator, we can fully describe the state of the total system at any time t [48] using the first and second moments of the field modes.

We define the following vector of operators

$$\hat{\mathbf{r}} = (\hat{x}_1, \hat{x}_2, \hat{p}_1, \hat{p}_2)^T, \quad (20)$$

where $\hat{x}_j = \sqrt{\frac{1}{2\omega}}(\hat{a}_j + \hat{a}_j^\dagger)$ and $\hat{p}_j = i\sqrt{\frac{1}{2\omega}}(\hat{a}_j^\dagger - \hat{a}_j)$ with $j = 1, 2$. The operators of the vector fulfill the commutation relations $[\hat{\mathbf{r}}, \hat{\mathbf{r}}^T] = iJ$, with $J = \begin{pmatrix} 0_2 & \mathbb{I}_2 \\ -\mathbb{I}_2 & 0_2 \end{pmatrix}$, where \mathbb{I}_2 and 0_2 are the identity matrix and the null matrix respectively. The state of the system is fully described by its statistical moments

$$\langle \hat{\mathbf{r}}_1 \dots \hat{\mathbf{r}}_4 \rangle = \text{Tr}\{\rho \hat{\mathbf{r}}_1 \dots \hat{\mathbf{r}}_4\}, \quad (21)$$

with first and second moments describing the Gaussian state. We construct the vector $|r\rangle$ of the first moments

$$|r\rangle = \sum_{i=1}^4 \langle \hat{\mathbf{r}}_i \rangle |i\rangle, \quad (22)$$

as well as the matrix made of the second moments of x and p :

$$V = \frac{1}{2} \sum_{i,j=1}^4 \langle \{\hat{\mathbf{r}}_i, \hat{\mathbf{r}}_j\} \rangle |i\rangle \langle j|. \quad (23)$$

The relationship between matrix V and the covariance matrix V_c is given by $V_c = V - |r\rangle \langle r|$. Therefore, in order to apply Krotov's method, we will use an object made of the elements of the vector of moments, the elements of the second moment matrix [63] and an independent parameter, which encodes all the information from the vector living in the infinite dimension Hilbert space. We will arrange it as follows

$$\psi = \begin{pmatrix} c \\ |r\rangle_1 \\ |r\rangle_2 \\ |r\rangle_3 \\ |r\rangle_4 \\ V_{11} \\ V_{12} \\ V_{13} \\ V_{14} \\ V_{22} \\ V_{23} \\ V_{24} \\ V_{33} \\ V_{34} \\ V_{44} \end{pmatrix}. \quad (24)$$

The evolution of our state ρ is given by

$$\frac{d\rho}{dt} = -i[H, \rho] + \mathcal{D}_T(\rho). \quad (25)$$

However, as we are interested in the evolution of the expectation values of the operators, we will resort to the Heisenberg equation. For any operator O , the evolution of its expectation value reads

$$\frac{d\langle O \rangle}{dt} = i\langle [H, O] \rangle + \langle \mathcal{D}_T^\dagger(O) \rangle, \quad (26)$$

where $\mathcal{D}_T^\dagger(O)$ is the adjoint dissipator and is given by

$$\begin{aligned} \mathcal{D}_T^\dagger(O) &= \gamma(N_b(T) + 1) \left(a^\dagger O a - \frac{1}{2} \{a^\dagger a, O\} \right) \\ &+ \gamma N_b(T) \left(a O a^\dagger - \frac{1}{2} \{a a^\dagger, O\} \right). \end{aligned} \quad (27)$$

Computing Eq. (26) for all the elements of Eq. (24) we can write the evolution as

$$\frac{\partial \psi}{\partial t} = A_f \psi, \quad (28)$$

which will be our Schrodinger-like equation of motion with the condition that $\psi(t=0) = \phi_i$, where ϕ_i is the initial state of the system rewritten in terms of first and second moments. Consequently, the backwards evolution of the co-states will be given by the adjoint Liouvillian dynamics

$$\frac{d\langle O \rangle}{dt} = i\langle [H, O] \rangle + \langle \mathcal{D}_T(O) \rangle, \quad (29)$$

where

$$\begin{aligned} \mathcal{D}_T(O) &= \gamma(N_b(T) + 1) \left(a O a^\dagger - \frac{1}{2} \{a^\dagger a, O\} \right) \\ &+ \gamma N_b(T) \left(a^\dagger O a - \frac{1}{2} \{a a^\dagger, O\} \right), \end{aligned} \quad (30)$$

and this will be translated to our Gaussian framework as

$$\frac{\partial \chi}{\partial t} = A_b \chi, \quad (31)$$

where it should be noted that the time runs backwards. The boundary condition in this case is $\chi(\tau) = \phi_t$, where ϕ_t is the target state and τ the final time of our evolution. The explicit forms of our A and A_B are deferred to the appendices.

Finally, the update of the field will be given by the derivative of the Liouvillian (multiplied by the imaginary unit) with respect to the field only. So, for the iteration i and for the control ϵ we have

$$\begin{aligned} \Delta \epsilon_i^i(t) &= \frac{S(t)}{\lambda_a} \text{Im} \left[\text{Tr} \left\{ \sigma^{i-1}(t) \frac{i \partial \mathcal{L}}{\partial \epsilon(t)} \Big|_{(i)} \rho^i(t) \right\} \right] \\ &= -\frac{S(t)}{\lambda_a} \text{Im} \left[\text{Tr} \left\{ \sigma^{i-1}(t) [\mu(a_1 + a_1^\dagger), \rho^i(t)] \right\} \right], \end{aligned} \quad (32)$$

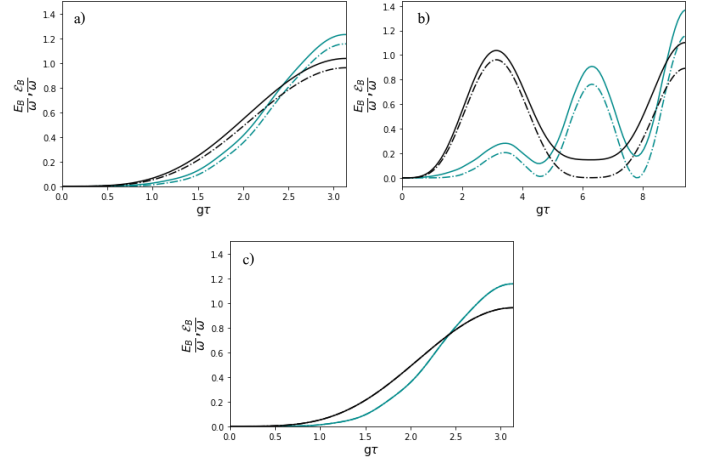


FIG. 4: Energy (dashed line) and ergotropy (dotted line) versus $g\tau$ in the case of optimizing the field and in the case of using an oscillatory field as in [43]. In a), maximal time was chosen such that for the non-optimized setting energy and ergotropy achieve their first maximums. In b), this time is doubled. We took $g = 0.2\omega$, $\gamma = 0.01\omega$, $F = \mu = 0.1\omega$, $N_b(T) = 1$ and $\kappa = 0.01$. c) shows the zero temperature case $N_b(T) = 0$, where the state remains pure. Ergotropy and energy take the same values, and correspond to values of ergotropy on plot a).

where ρ and σ represent the density matrix of the forward and backward state respectively. This update can be calculated explicitly for any given pair of states and the result is a function of the elements of $\bar{\mathbf{r}}$ and V (see appendix). Therefore, for any pair of ψ and χ objects, Eq. (32) is defined.

Numerical results of our optimization and the non-optimized case are both plotted in Fig. 4a and it is seen that for the optimized pulse the energy and ergotropy are higher. The energy spent by the optimized laser pulse is 30.73 while by the oscillatory pulse 31.41. In Fig. 4b it is seen that for longer times more energy can be transferred to the battery in both optimized and non-optimized process. As longer time offers bigger opportunities for optimization of the field pulse, the energy cost increase is modest (36.7), compared to 94.25 with the fixed sinusoidal pulse.

One should note that, for initial state of the charger-battery system being $|0\rangle_C \otimes |0\rangle_B$, the equation of motion (28) implies that, for a fixed driving $\epsilon(t)$ at temperature T , the ergotropy of the final state does not depend on temperature, following the separation of energy of the target state into parts which depend separately on driving and temperature:

$$\mathcal{E}_{\epsilon(t),T} = E_{\epsilon(t),T=0} = E_{\epsilon(t),T} - E_{\epsilon(t)=0,T}. \quad (33)$$

The proof of (33) runs analogously to the one in [43] for a fixed, sinusoidal driving. It relies on the fact that for quadratic Hamiltonians and a lossy channel at tem-

perature $T = 0$, the initial vacuum state evolves into a product of coherent states.

From there, it is easy to see how our algorithm could be used in finding optimal driving of a harmonic oscillator battery. Namely, we run the algorithm for target states which have the desired ergotropy, and select the pulse which has the lowest energy cost. (33) guarantees that this pulse will lead to a state with the same ergotropy when applied at an arbitrary temperature T . Moreover, this pulse optimizes the ratio $\frac{\mathcal{E}}{E}$ for every temperature, as every other pulse with the same energy cost has non-greater \mathcal{E} , while $E_{\epsilon(t)=0,T}$, which is the only value that changes the energy E depends only on the temperature.

Nevertheless, the method we introduced can be used also for cases which require field optimization over mixed state evolution. We expect this to be crucial for physically realistic settings, in which the initial state cannot be taken as vacuum, or for quadratic interaction with the field.

VI. REALIZATION

Both the qubit-qubit and oscillator-oscillator models discussed above can be implemented with the current superconducting quantum technology [49]. The architecture is easily scalable to multiple qubit and/or resonator configurations. The chip integration allows coupled multiple transmon qubits or resonator-resonator designs with ultimately stable operations [50]. The in-situ tunable couplings can be realized using modular capacitive [51] or inductive [52–54] coupling with a large on to off coupling ratio reaching up to GHz ranges. Each qubit or resonator in the chain can also be individually controlled by coupling them to a 1D transmission line or waveguide. Note that, the coupling can be short (capacitive) or long (inductive) range, allowing multiple quantum units (resonators or qubits) to efficiently interact; necessary condition to implement the current quantum control proposal. Additionally, the microwave control electronics and control methods of these quantum circuits haven been extensively improved and developed over the last few years [55–57]. Proper pulse shaping allows faster operations, reducing the gate errors, or improving the gate fidelity. For instance, open or close-loop optimal control methods [58] allow stable gate operations by optimizing several parameters related to the shape, amplitude, phase, and other properties of the control field acting on the quantum units.

VII. CONCLUSIONS

In this paper, we investigated optimized protocols for charging quantum batteries, motivated by the fact that, as far as we know, the current literature focuses on simple sinusoidal charging field. Apart from maximising the fidelity with respect to a desired target state, while min-

imising the energy spent, we also took into the account the turning on and off of the field to make our results experimentally feasible.

Firstly, we studied the case in which both the charger and the battery are two two-level systems. Although the achieved values of ergotropy are similar to the non-optimized case, optimization allows for a significant reduction of the energy needed to charge the battery. A difference between values of ergotropy and energy stored increases with growing number of cells constituting the battery. We observe that for 4 cells, while our results are better in terms of energy and ergotropy, the optimized pulse requires more energy. That is because performing the optimization and at the same time minimizing the energy used by the field is not numerically stable. We conjecture that with higher computational power the optimization could be carried more efficiently, resulting in pulses with lower energy costs.

Secondly, we move to the case in which charger and battery are oscillators. To do so, within the Gaussian formalism we devised a framework to perform the optimization for infinite dimension systems, without putting an arbitrary limit on the dimensionality of the subspace taken into account in the optimization. In this case, the results show significant improvement both in terms of ergotropy and energy cost. In the idealized scenario of the vacuum initial state of the charger and battery, the setting enables us to connect optimal field pulses leading to high ergotropy/energy ratios with optimal strategies in zero temperature regime. The method itself however is general, and can be used to perform optimization for an arbitrary temperature.

The infinite dimensional systems optimization method introduced here paves the way to investigate more interesting cases, such as batteries made of more than one oscillator, interacting between each other. This could foster the understanding of the role of the geometry in the optimization.

Acknowledgements

RRR and GS acknowledge Michael Goerz and Daniel Reich for fruitful discussions. BA would like to acknowledge Tomasz Linowski for his useful arguments. We acknowledge support from the Foundation for Polish Science through IRAP project co-financed by EU within the Smart Growth Operational Programme (contract no.2018/MAB/5). S.B. acknowledges funding by the Natural Sciences and Engineering Research Council of Canada (NSERC) through its Discovery Grant, funding and advisory support provided by Alberta Innovates through the Accelerating Innovations into CarE (AICE) – Concepts Program, and support from Alberta Innovates and NSERC through Advance Grant.

VIII. APPENDICES

A. Energy used by the field

In order to obtain the interaction Hamiltonian $H_I(t)$ in (15) the classical oscillatory field is assumed to be of the form

$$\epsilon(t) = E_0 \cos \omega t = \frac{E_0}{2} (e^{i\omega t} + e^{-i\omega t}), \quad (34)$$

where E_0 is the constant amplitude of the field. In the dipole approximation the interaction Hamiltonian $H_I(t)$ is then written as [59]

$$\begin{aligned} H_I(t) &= \mu \epsilon(t) \sigma^x \\ &= \frac{\mu E_0}{2} (e^{i\omega t} + e^{-i\omega t}) \sigma^x, \end{aligned} \quad (35)$$

where μ is the coupling constant and σ^x the Pauli operator. Using the equality $\sigma^x = \sigma^+ + \sigma^-$ where σ^\pm are the raising and lowering operators and applying the RWA approximation we get

$$\begin{aligned} H_I(t) &= \frac{\mu E_0}{2} (e^{i\omega t} \sigma^+ + e^{-i\omega t} \sigma^-) \\ &= F (e^{i\omega t} \sigma^+ + e^{-i\omega t} \sigma^-), \end{aligned} \quad (36)$$

which is the interaction Hamiltonian in Eq. (15). Therefore choosing $E_0 = 2$ we have $F = \mu$. And the energy spent by the oscillatory field is then computed as

$$\begin{aligned} \mathcal{W}_\tau &= \int_0^\tau dt |\epsilon(t)|^2 \\ &= \int_0^\tau dt 4 \cos^2(\omega t) \\ &= 2\tau + \frac{\sin(2\omega\tau)}{\omega}. \end{aligned} \quad (37)$$

B. Equations of motion

The Krotov method for dissipative systems has been studied before, for instance in Refs. [60, 61], it has been established that in this case, the forward and backward equations are:

$$\frac{d\rho_F}{dt} = -i[H, \rho_F] + \mathcal{D}_T(\rho_F) \quad (38)$$

$$\frac{d\rho_B}{dt} = -i[H, \rho_B] - \mathcal{D}_T^\dagger(\rho_B) \quad (39)$$

Where

$$\mathcal{D}_T^\dagger(\rho) = \sum_k (A_k^\dagger \rho A_k - \frac{1}{2} A_k^\dagger A_k \rho - \frac{1}{2} \rho A_k^\dagger A_k) \quad (40)$$

and

$$\mathcal{D}_T(\rho) = \sum_k (A_k \rho A_k^\dagger - \frac{1}{2} A_k^\dagger A_k \rho - \frac{1}{2} \rho A_k^\dagger A_k) \quad (41)$$

In order to compute the evolution of an observable we compute the so called ‘‘adjoint’’ master equation for both the forward and backwards evaluations, which just means computing $\langle O_i \rangle = Tr[O \rho_i]$, where i =forward, backwards which results in:

$$\frac{d\langle O_F \rangle}{dt} = i\langle [H, O_F] \rangle + \langle \mathcal{D}_T^\dagger(O_F) \rangle \quad (42)$$

$$\frac{d\langle O_B \rangle}{dt} = i\langle [H, O_B] \rangle - \langle \mathcal{D}_T(O_B) \rangle \quad (43)$$

Since for Gaussian systems all of the evolution can be quantified using the vector of first moments and the matrix of second moments, we just need to compute the evolution of the observables that appear as the components of the vector (24) which evolves according to the dynamical Eq. (31) where A_f is given by:

$$A_f = \begin{pmatrix} 0 & 0 & 0 & 0 & 0 & 0 & 0 & 0 & 0 & 0 & 0 & 0 & 0 & 0 & 0 & 0 & 0 & 0 & 0 & 0 \\ 0 & -\frac{\gamma}{2} & 0 & \frac{g}{w} & \frac{g}{w} & 0 & 0 & 0 & 0 & 0 & 0 & 0 & 0 & 0 & 0 & 0 & 0 & 0 & 0 & 0 \\ 0 & 0 & 0 & \frac{g}{w} & 1 & 0 & 0 & 0 & 0 & 0 & 0 & 0 & 0 & 0 & 0 & 0 & 0 & 0 & 0 & 0 \\ \sqrt{2w\mu\epsilon(t)} & -w^2 & -gw & -\frac{\gamma}{2} & 0 & 0 & 0 & 0 & 0 & 0 & 0 & 0 & 0 & 0 & 0 & 0 & 0 & 0 & 0 & 0 \\ 0 & -gw & -w^2 & 0 & 0 & 0 & 0 & 0 & 0 & 0 & 0 & 0 & 0 & 0 & 0 & 0 & 0 & 0 & 0 & 0 \\ \frac{\gamma(n+\frac{1}{2})}{w} & 0 & 0 & 0 & 0 & -\gamma & 0 & 2 & \frac{2g}{w} & 0 & 0 & 0 & 0 & 0 & 0 & 0 & 0 & 0 & 0 & 0 \\ 0 & 0 & 0 & 0 & 0 & 0 & -\frac{\gamma}{2} & \frac{g}{w} & 1 & 0 & 0 & 1 & \frac{g}{w} & 0 & 0 & 0 & 0 & 0 & 0 & 0 \\ 0 & \sqrt{2w\mu\epsilon(t)} & 0 & 0 & 0 & -w^2 & -gw & -\gamma & 0 & 0 & 0 & 0 & 0 & 1 & \frac{g}{w} & 0 & 0 & 0 & 0 & 0 \\ 0 & 0 & 0 & 0 & 0 & -gw & -w^2 & 0 & -\frac{\gamma}{2} & 0 & 0 & 0 & 0 & 0 & 1 & \frac{g}{w} & 0 & 0 & 0 & 0 \\ 0 & 0 & 0 & 0 & 0 & 0 & 0 & 0 & 0 & 0 & 0 & 0 & \frac{2g}{w} & 2 & 0 & 0 & 0 & 0 & 0 & 0 \\ 0 & 0 & 0 & 0 & 0 & 0 & -w^2 & 0 & 0 & -gw & -\frac{\gamma}{2} & 0 & -gw & 0 & \frac{g}{w} & 1 & 0 & 0 & 0 & 0 \\ 0 & 0 & \sqrt{2w\mu\epsilon(t)} & 0 & 0 & 0 & -gw & 0 & 0 & -w^2 & 0 & 0 & 0 & 0 & \frac{g}{w} & 1 & 0 & 0 & 0 & 0 \\ 0 & 0 & 0 & 0 & 0 & 0 & -gw & 0 & 0 & -w^2 & 0 & 0 & 0 & 0 & \frac{g}{w} & 1 & 0 & 0 & 0 & 0 \\ \gamma w(n+\frac{1}{2}) & 0 & 0 & 2\sqrt{2w\mu\epsilon(t)} & 0 & 0 & 0 & -2w^2 & 0 & 0 & -2gw & 0 & -\gamma & 0 & 0 & 0 & 0 & 0 & 0 & 0 \\ 0 & 0 & 0 & 0 & \sqrt{2w\mu\epsilon(t)} & 0 & 0 & 0 & -gw & -w^2 & 0 & -w^2 & -gw & 0 & -\frac{\gamma}{2} & 0 & 0 & 0 & 0 & 0 \\ 0 & 0 & 0 & 0 & 0 & 0 & 0 & 0 & -2gw & 0 & 0 & -2w^2 & 0 & 0 & -2w^2 & 0 & 0 & 0 & 0 & 0 \end{pmatrix} \quad (44)$$

In the same way the matrix that defines the backward

evolution is given by:

$$A_b = \begin{pmatrix} 0 & 0 & 0 & 0 & 0 & 0 & 0 & 0 & 0 & 0 & 0 & 0 & 0 & 0 & 0 & 0 & 0 & 0 & 0 & 0 \\ 0 & -\frac{3\gamma}{2} & 0 & 1 & \frac{g}{w} & 0 & 0 & 0 & 0 & 0 & 0 & 0 & 0 & 0 & 0 & 0 & 0 & 0 & 0 & 0 \\ 0 & 0 & -\gamma & \frac{g}{w} & 1 & 0 & 0 & 0 & 0 & 0 & 0 & 0 & 0 & 0 & 0 & 0 & 0 & 0 & 0 & 0 \\ -\sqrt{2w}\epsilon(t)\mu & -w^2 & -gw & -\frac{3\gamma}{2} & 0 & 0 & 0 & 0 & 0 & 0 & 0 & 0 & 0 & 0 & 0 & 0 & 0 & 0 & 0 & 0 \\ 0 & -gw & -w^2 & 0 & -\gamma & 0 & 0 & 0 & 0 & 0 & 0 & 0 & 0 & 0 & 0 & 0 & 0 & 0 & 0 & 0 \\ -\frac{\gamma(n+\frac{1}{2})}{w} & 0 & 0 & 0 & 0 & -2\gamma & 0 & 2 & \frac{2g}{w} & 0 & 0 & 0 & 0 & 0 & 0 & 0 & 0 & 0 & 0 & 0 \\ 0 & 0 & 0 & 0 & 0 & 0 & -\frac{3\gamma}{2} & \frac{g}{w} & 1 & 0 & 1 & \frac{g}{w} & 0 & 0 & 0 & 0 & 0 & 0 & 0 & 0 \\ 0 & -\sqrt{2w}\epsilon(t)\mu & 0 & 0 & 0 & -w^2 & -gw & -2\gamma & 0 & 0 & 0 & 0 & 1 & \frac{g}{w} & 0 & 0 & 0 & 0 & 0 & 0 \\ 0 & 0 & 0 & 0 & 0 & -gw & -w^2 & 0 & -\frac{3\gamma}{2} & 0 & 0 & 0 & 0 & 0 & 1 & \frac{g}{w} & 0 & 0 & 0 & 0 \\ 0 & 0 & 0 & 0 & 0 & 0 & 0 & 0 & 0 & -\gamma & \frac{2g}{w} & 2 & 0 & 0 & 0 & 0 & 0 & 0 & 0 & 0 \\ 0 & 0 & 0 & 0 & 0 & 0 & 0 & 0 & 0 & 0 & 0 & 0 & 0 & 0 & 0 & 0 & 0 & 0 & 0 & 0 \\ 0 & 0 & -\sqrt{2w}\epsilon(t)\mu & 0 & 0 & 0 & -w^2 & 0 & 0 & -gw & -\frac{3\gamma}{2} & 0 & \frac{g}{w} & 1 & 0 & 0 & 0 & 0 & 0 & 0 \\ 0 & 0 & 0 & 0 & 0 & 0 & -gw & 0 & 0 & -w^2 & 0 & -\gamma & 0 & \frac{g}{w} & 1 & 0 & 0 & 0 & 0 & 0 \\ -\gamma w(n+\frac{1}{2}) & 0 & 0 & -2\sqrt{2w}\epsilon(t)\mu & 0 & 0 & 0 & -2w^2 & 0 & 0 & -2gw & 0 & -2\gamma & 0 & 0 & 0 & 0 & 0 & 0 & 0 \\ 0 & 0 & 0 & 0 & -\sqrt{2w}\epsilon(t)\mu & 0 & 0 & 0 & -gw & -w^2 & 0 & -w^2 & -gw & 0 & -\frac{3\gamma}{2} & 0 & 0 & 0 & 0 & 0 \\ 0 & 0 & 0 & 0 & 0 & 0 & 0 & 0 & 0 & -2gw & 0 & 0 & -2w^2 & 0 & 0 & 0 & 0 & 0 & 0 & -\gamma \end{pmatrix} \quad (45)$$

One may notice that the difference between both matrices is merely a shift on the diagonal and part of

the “constant” terms, to see this better consider $M := A_f - A_b$:

$$M = \begin{pmatrix} 0 & 0 & 0 & 0 & 0 & 0 & 0 & 0 & 0 & 0 & 0 & 0 & 0 & 0 & 0 & 0 & 0 & 0 & 0 & 0 \\ 0 & \gamma & 0 & 0 & 0 & 0 & 0 & 0 & 0 & 0 & 0 & 0 & 0 & 0 & 0 & 0 & 0 & 0 & 0 & 0 \\ 0 & 0 & \gamma & 0 & 0 & 0 & 0 & 0 & 0 & 0 & 0 & 0 & 0 & 0 & 0 & 0 & 0 & 0 & 0 & 0 \\ 0 & 0 & 0 & \gamma & 0 & 0 & 0 & 0 & 0 & 0 & 0 & 0 & 0 & 0 & 0 & 0 & 0 & 0 & 0 & 0 \\ 0 & 0 & 0 & 0 & \gamma & 0 & 0 & 0 & 0 & 0 & 0 & 0 & 0 & 0 & 0 & 0 & 0 & 0 & 0 & 0 \\ \frac{2\gamma(n+\frac{1}{2})}{w} & 0 & 0 & 0 & 0 & \gamma & 0 & 0 & 0 & 0 & 0 & 0 & 0 & 0 & 0 & 0 & 0 & 0 & 0 & 0 \\ 0 & 0 & 0 & 0 & 0 & 0 & \gamma & 0 & 0 & 0 & 0 & 0 & 0 & 0 & 0 & 0 & 0 & 0 & 0 & 0 \\ 0 & 0 & 0 & 0 & 0 & 0 & 0 & \gamma & 0 & 0 & 0 & 0 & 0 & 0 & 0 & 0 & 0 & 0 & 0 & 0 \\ 0 & 0 & 0 & 0 & 0 & 0 & 0 & 0 & \gamma & 0 & 0 & 0 & 0 & 0 & 0 & 0 & 0 & 0 & 0 & 0 \\ 0 & 0 & 0 & 0 & 0 & 0 & 0 & 0 & 0 & \gamma & 0 & 0 & 0 & 0 & 0 & 0 & 0 & 0 & 0 & 0 \\ 0 & 0 & 0 & 0 & 0 & 0 & 0 & 0 & 0 & 0 & \gamma & 0 & 0 & 0 & 0 & 0 & 0 & 0 & 0 & 0 \\ 2\gamma w(n+\frac{1}{2}) & 0 & 0 & 0 & 0 & 0 & 0 & 0 & 0 & 0 & 0 & 0 & 0 & \gamma & 0 & 0 & 0 & 0 & 0 & 0 \\ 0 & 0 & 0 & 0 & 0 & 0 & 0 & 0 & 0 & 0 & 0 & 0 & 0 & 0 & \gamma & 0 & 0 & 0 & 0 & 0 \\ 0 & 0 & 0 & 0 & 0 & 0 & 0 & 0 & 0 & 0 & 0 & 0 & 0 & 0 & 0 & \gamma & 0 & 0 & 0 & 0 \end{pmatrix}. \quad (46)$$

To see the general form of M (without going element by element), we just need to compute the difference between the dissipative parts of the backward and forward equations.

The dissipator for the backward equation is

$$\begin{aligned} \mathcal{D}_T^\dagger(O) &= \gamma(N_b + 1) \left(a^\dagger O a - \frac{1}{2} \{a^\dagger a, O\} \right) \\ &+ \gamma N_b \left(a O a^\dagger - \frac{1}{2} \{a a^\dagger, O\} \right) \end{aligned} \quad (47)$$

and for the forward

$$\begin{aligned} \mathcal{D}_T(O) &= \gamma(N_b + 1) \left(a O a^\dagger - \frac{1}{2} \{a^\dagger a, O\} \right) \\ &+ \gamma N_b \left(a^\dagger O a - \frac{1}{2} \{a a^\dagger, O\} \right). \end{aligned} \quad (48)$$

Since there is a minus sign in the backwards evolution the difference in the dynamics is given by the sum of these generators:

$$\begin{aligned} \mathcal{D}_T(O) + \mathcal{D}_T^\dagger(O) &= \gamma N_b (a^\dagger O a + a O a^\dagger - \{a a^\dagger, O\}) \\ &+ \gamma(N_b + 1) (a^\dagger O a + a O a^\dagger - \{a^\dagger a, O\}) \end{aligned} \quad (49)$$

We may rewrite Eq. (49) by using the equality:

$$\begin{aligned} a^\dagger O a + a O a^\dagger - a a^\dagger O - O a a^\dagger &= a[O, a^\dagger] + [a^\dagger, O] a \\ &= a[O, a^\dagger] - [O, a^\dagger] a + O \\ &= [a, [O, a^\dagger]] - O \end{aligned} \quad (50)$$

Similarly one may obtain:

$$a^\dagger O a + a O a^\dagger - a^\dagger a O - O a^\dagger a = [a^\dagger, [O, a]] + O \quad (51)$$

So that one may write:

$$\begin{aligned}
\mathcal{D}_T(O) + \mathcal{D}_T^\dagger(O) &= \gamma N_b ([a, [O, a^\dagger]] - O) \\
&+ \gamma(N_b + 1) ([a^\dagger, [O, a]] + O) \\
&= \gamma N_b ([a, [O, a^\dagger]] + [a^\dagger, [O, a]]) \\
&+ \gamma ([a^\dagger, [O, a]] + O) \quad (52)
\end{aligned}$$

This expression serves to construct the backwards from the forward equation, since we care about the evolution of observables in X, P it is more comfortable to write this as:

$$\begin{aligned}
\mathcal{D}_T(O) + \mathcal{D}_T^\dagger(O) &= \gamma N_b w \left([X_1, [O, X_1]] + \frac{1}{w^2} [P_1, [O, P_1]] \right) \quad \text{and} \\
&+ \gamma \frac{w}{2} \left([X_1, [O, X_1]] + \frac{1}{w^2} [P_1, [O, P_1]] \right) \\
&+ \frac{i}{w} ([X_1, [O, P_1]] - [P_1, [O, X_1]]) + \gamma O, \quad (53)
\end{aligned}$$

Which allows to compute the backwards evolution from the forward straight-forwardly. For instance let us consider X_1 and X_1^2

$$[X_1, P_1] = i \quad (54)$$

$$[X_1^2, P_1] = 2iX_1 \quad (55)$$

$$[P_1, [X_1, P_1]] = 0 \quad (56)$$

$$[P_1, [X_1^2, P_1]] = 2 \quad (57)$$

substituting those relations in Eq. (53) one obtains:

$$\langle \mathcal{D}_T(X_1) + \mathcal{D}_T^\dagger(X_1) \rangle = \gamma \langle X_1 \rangle, \quad (58)$$

$$\langle \mathcal{D}_T(X_1^2) + \mathcal{D}_T^\dagger(X_1^2) \rangle = \gamma \langle X_1^2 \rangle + \frac{2\gamma}{w} \left(n + \frac{1}{2} \right). \quad (59)$$

Results that agree with computing all of the equations of motion for both the forward and backward equations.

C. Explicit calculation of the trace of Eq. (32)

Any two-mode Gaussian state can be written as [48]

$$\rho = \frac{1}{(2\pi)^2} \int_{\mathbb{R}^4} d\mathbf{r} \chi_G(\mathbf{r}) \hat{D}_{\mathbf{r}}, \quad (60)$$

with the characteristic function

$$\chi_G(\mathbf{r}) = e^{-\frac{1}{2} \mathbf{r}^\top \Omega^\top V_c \Omega \mathbf{r} + i \mathbf{r}^\top \Omega^\top \bar{\mathbf{r}}} \quad (61)$$

$$\hat{D}_{\mathbf{r}} = e^{i \mathbf{r}^\top \Omega \mathbf{r}} \quad (62)$$

in which $\mathbf{r} = [x_1, p_1, x_2, p_2]$, V_c is the covariance matrix with entries $V_{c\{i,j\}} = \text{Tr} \left\{ \rho \left(\frac{1}{2} (\mathbf{r}_i \mathbf{r}_j + \mathbf{r}_j \mathbf{r}_i) \right) \right\} - \bar{\mathbf{r}}_i \bar{\mathbf{r}}_j$, and $[\bar{\mathbf{r}}]_i = \text{Tr} \{ \rho \mathbf{r}_i \}$. Defining $\mathbf{r}_i = [x_i, p_i]$ we have

$$\mathbf{r} = \mathbf{r}_1 \oplus \mathbf{r}_2, \quad (63)$$

which implies

$$D_{\mathbf{r}} = D_{\mathbf{r}_1} \otimes D_{\mathbf{r}_2}. \quad (64)$$

In the calculation we will also use identity expansion (on the two mode space and also the fact that all our simulations have been done with $\omega = 1$) in the basis of one-mode coherent states:

$$\mathbb{1} = \frac{1}{2\pi} \int d\tilde{x}_1 d\tilde{p}_1 \left| \frac{\tilde{x}_1 + i\tilde{p}_1}{\sqrt{2}} \right\rangle \left\langle \frac{\tilde{x}_1 + i\tilde{p}_1}{\sqrt{2}} \right| \otimes \mathbb{1}_2, \quad (65)$$

where we explicitly used a representation of a coherent single mode state $|\alpha\rangle = \left| \frac{\tilde{x}_1 + i\tilde{p}_1}{\sqrt{2}} \right\rangle$.

By denoting by $\chi_G(\mathbf{r}')$ the characteristic function of the state σ (see Eq. (60)), we obtain

$$\begin{aligned}
\text{Tr}(\sigma(a_1 + a_1^\dagger)\rho) &= \text{Tr}(\sigma(a_1 + a_1^\dagger)\rho^\dagger) \\
&= \frac{1}{(2\pi)^4} \text{Tr} \left(\int_{\mathbb{R}^4} d\mathbf{r} \int_{\mathbb{R}^4} d\mathbf{r}' \chi_G^*(\mathbf{r}) \chi_G(\mathbf{r}') D_{\mathbf{r}'} (a_1 + a_1^\dagger) D_{-\mathbf{r}} \right) \\
&= \frac{1}{(2\pi)^5} \int_{\mathbb{R}^4} d\mathbf{r} \int_{\mathbb{R}^4} d\mathbf{r}' \chi_G^*(\mathbf{r}) \chi_G(\mathbf{r}') \int_{\mathbb{R}^2} d\tilde{x}_1 d\tilde{p}_1 \left(\text{Tr}(D_{\mathbf{r}'} a_1 |\alpha\rangle \langle \alpha| D_{-\mathbf{r}}) + \text{Tr}(D_{\mathbf{r}'} |\alpha\rangle \langle \alpha| a_1^\dagger D_{-\mathbf{r}}) \right) \\
&= \frac{1}{(2\pi)^5} \int_{\mathbb{R}^4} d\mathbf{r} \int_{\mathbb{R}^4} d\mathbf{r}' \chi_G^*(\mathbf{r}) \chi_G(\mathbf{r}') \int_{\mathbb{R}^2} d\tilde{x}_1 d\tilde{p}_1 \sqrt{2} \tilde{x}_1 \langle \alpha | D_{-\mathbf{r}_1} D_{\mathbf{r}'_1} | \alpha \rangle \text{Tr}(D_{-\mathbf{r}_2} D_{\mathbf{r}'_2}), \quad (66)
\end{aligned}$$

where we exploited $a_1 |\alpha\rangle = \frac{x_1 + ip_1}{\sqrt{2}} |\alpha\rangle$. Upon utilising

$$\text{Tr}(D_{-\mathbf{r}_2} D_{\mathbf{r}'_2}) = 2\pi \delta(-\mathbf{r}_2 + \mathbf{r}'_2) = 2\pi \delta(-x_2 + x'_2) \delta(-p_2 + p'_2), \quad (67)$$

$$D_\alpha |0\rangle = |\alpha\rangle, \quad (68)$$

$$D_\alpha D_\beta = e^{\alpha\beta^* - \alpha^*\beta} D_\beta D_\alpha, \quad (69)$$

$$\langle \alpha | \beta \rangle = e^{-\frac{|\alpha|^2 + |\beta|^2 - 2\alpha^*\beta}{2}}, \quad (70)$$

we obtain

$$\begin{aligned} \text{Tr}(\sigma(a_1 + a_1^\dagger)\rho) &= \frac{\sqrt{2}}{(2\pi)^4} \int_{\mathbb{R}^4} \mathbf{dr} \int dx'_1 dp'_1 \int d\tilde{x}_1 d\tilde{p}_1 \chi_G(x_1, p_1, x_2, p_2) \chi_G^*(x'_1, p'_1, x_2, p_2) \tilde{x}_1 \langle \alpha | D_{-\mathbf{r}_1} D_{\mathbf{r}'_1} | \alpha \rangle = \\ &= \frac{\sqrt{2}}{(2\pi)^4} \int dx_1 dp_1 dx_2 dp_2 dx'_1 dp'_1 d\tilde{x}_1 d\tilde{p}_1 \chi_G(x_1, p_1, x_2, p_2) \chi_G^*(x'_1, p'_1, x_2, p_2) \\ &\quad \tilde{x}_1 e^{-\frac{1}{2}(\frac{x_1^2 + p_1^2 + x_2^2 + p_2^2}{2}) - x_1 x'_1 - p_1 p'_1 + i(x_1 p'_1 - x'_1 p_1 + \tilde{x}_1(p'_1 - p_1) + \tilde{p}_1(x'_1 - x_1))}. \end{aligned} \quad (71)$$

This integral can be solved analytically (we solved it using Mathematica) and the solution will be in terms

of first moments and the elements of the the covariance matrix V_c of the two states.

-
- [1] Strasberg P, Winter A. First and Second Law of Quantum Thermodynamics: A Consistent Derivation Based on a Microscopic Definition of Entropy. PRX Quantum. 2021 Aug;2:030202. Available from: <https://link.aps.org/doi/10.1103/PRXQuantum.2.030202>.
- [2] Brandão FGSL, Horodecki M, Ng NHY, Oppenheim J, Wehner S. The second laws of quantum thermodynamics. Proc Natl Acad Sci USA. 2015;112:3275. Available from: <https://doi.org/10.1073/pnas.1411728112>.
- [3] Esposito M, den Broeck CV. Second law and Landauer principle far from equilibrium. EPL (Europhysics Letters). 2011 aug;95(4):40004. Available from: <https://doi.org/10.1209/2F0295-5075%2F95%2F40004>.
- [4] Lobejko M. The tight Second Law inequality for coherent quantum systems and finite-size heat baths. Nature Communications. 2021 feb;12(1). Available from: <https://doi.org/10.1038%2Fs41467-021-21140-4>.
- [5] Uzdin R, Levy A, Kosloff R. Equivalence of Quantum Heat Machines, and Quantum-Thermodynamic Signatures. Phys Rev X. 2015 Sep;5:031044. Available from: <https://link.aps.org/doi/10.1103/PhysRevX.5.031044>.
- [6] Uzdin R. Coherence-Induced Reversibility and Collective Operation of Quantum Heat Machines via Coherence Recycling. Phys Rev Applied. 2016 Aug;6:024004. Available from: <https://link.aps.org/doi/10.1103/PhysRevApplied.6.024004>.
- [7] Klatzow J, Becker JN, Ledingham PM, Weinzetl C, Kaczmarek KT, Saunders DJ, et al. Experimental Demonstration of Quantum Effects in the Operation of Microscopic Heat Engines. Phys Rev Lett. 2019 Mar;122:110601. Available from: <https://link.aps.org/doi/10.1103/PhysRevLett.122.110601>.
- [8] Kosloff R. Quantum thermodynamics and open-systems modeling. The Journal of Chemical Physics. 2019;150(20):204105. Available from: <https://doi.org/10.1063/1.5096173>.
- [9] Gelbwaser-Klimovsky D, Alicki R, Kurizki G. Minimal universal quantum heat machine. Phys Rev E. 2013 Jan;87:012140. Available from: <https://link.aps.org/doi/10.1103/PhysRevE.87.012140>.
- [10] Brask JB, Haack G, Brunner N, Huber M. Autonomous quantum thermal machine for generating steady-state entanglement. New Journal of Physics. 2015 nov;17(11):113029. Available from: <https://doi.org/10.1088/1367-2630/17/11/113029>.
- [11] Correa LA, Palao JP, Alonso D, Adesso G. Quantum-enhanced absorption refrigerators. Scientific Reports. 2014 feb;4(1). Available from: <https://doi.org/10.1038%2Fsrep03949>.
- [12] Dann R, Kosloff R, Salamon P. Quantum Finite-Time Thermodynamics: Insight from a Single Qubit Engine. Entropy. 2020 nov;22(11):1255. Available from: <https://doi.org/10.3390%2Fentropy22111255>.
- [13] Bhattarjee S, Dutta A. Quantum thermal machines and batteries. The European Physical Journal B. 2021 dec;94(12). Available from: <https://doi.org/10.1140%2Fepjb%2Fs10051-021-00235-3>.
- [14] Ng NHY, Woods MP. Resource Theory of Quantum Thermodynamics: Thermal Operations and Second Laws. In: Fundamental Theories of Physics. Springer International Publishing; 2018. p. 625–650. Available from: https://doi.org/10.1007%2F978-3-319-99046-0_26.
- [15] Sparaciari C, Oppenheim J, Fritz T. Resource theory for work and heat. Physical Review A. 2017 nov;96(5). Available from: <https://doi.org/10.1103%2Fphysreva.96.052112>.
- [16] Shi YH, Shi HL, Wang XH, Hu ML, Liu SY, Yang WL, et al. Quantum coherence in a quantum heat engine. Journal of Physics A: Mathematical and Theoretical. 2020 jan;53(8):085301. Available from: <https://doi.org/10.1088%2F1751-8121%2F53%2F085301>.
- [17] Lobejko M, Mazurek P, Horodecki M. Thermodynamics of Minimal Coupling Quantum Heat Engines. Quantum. 2020 dec;4:375. Available from: <https://doi.org/10.22331%2Fq-2020-12-23-375>.
- [18] Biswas T, Lobejko M, Mazurek P, Jawiecki K, Horodecki M. Extraction of ergotropy: free energy bound and ap-

- plication to open cycle engines. arXiv; 2022. Available from: <https://arxiv.org/abs/2205.06455>.
- [19] Campisi M, Pekola J, Fazio R. Nonequilibrium fluctuations in quantum heat engines: theory, example, and possible solid state experiments. *New Journal of Physics*. 2015 mar;17(3):035012. Available from: <https://doi.org/10.1088/1367-2630/17/3/035012>.
- [20] Zhang K, Bariani F, Meystre P. Quantum Optomechanical Heat Engine. *Phys Rev Lett*. 2014 Apr;112:150602. Available from: <https://link.aps.org/doi/10.1103/PhysRevLett.112.150602>.
- [21] Gelbwaser-Klimovsky D, Kurizki G. Work extraction from heat-powered quantized optomechanical setups. 2014. Available from: <https://arxiv.org/abs/1410.8561>.
- [22] Roßnagel J, Dawkins ST, Tolazzi KN, Abah O, Lutz E, Schmidt-Kaler F, et al. A single-atom heat engine. *Science*. 2016 apr;352(6283):325–329. Available from: <https://doi.org/10.1126/Science.aad6320>.
- [23] Maslennikov G, Ding S, Hablützel R, Gan J, Roulet A, Nimmrichter S, et al. Quantum absorption refrigerator with trapped ions. *Nature Communications*. 2019 jan;10(1). Available from: <https://doi.org/10.1038/2Fs41467-018-08090-0>.
- [24] von Lindensfeld D, Gräß O, Schmiegelow CT, Kaushal V, Schulz J, Mitchison MT, et al. Spin Heat Engine Coupled to a Harmonic-Oscillator Flywheel. *Phys Rev Lett*. 2019 Aug;123:080602. Available from: <https://link.aps.org/doi/10.1103/PhysRevLett.123.080602>.
- [25] Andolina GM, Farina D, Mari A, Pellegrini V, Giovannetti V, Polini M. Charger-mediated energy transfer in exactly solvable models for quantum batteries. *Phys Rev B*. 2018 Nov;98:205423. Available from: <https://link.aps.org/doi/10.1103/PhysRevB.98.205423>.
- [26] Andolina GM, Keck M, Mari A, Campisi M, Giovannetti V, Polini M. Extractable Work, the Role of Correlations, and Asymptotic Freedom in Quantum Batteries. *Phys Rev Lett*. 2019 Feb;122:047702. Available from: <https://link.aps.org/doi/10.1103/PhysRevLett.122.047702>.
- [27] Alicki R, Fannes M. Entanglement boost for extractable work from ensembles of quantum batteries. *Phys Rev E*. 2013 Apr;87:042123. Available from: <https://link.aps.org/doi/10.1103/PhysRevE.87.042123>.
- [28] Hovhannisyán KV, Perarnau-Llobet M, Huber M, Acín A. Entanglement Generation is Not Necessary for Optimal Work Extraction. *Phys Rev Lett*. 2013 Dec;111:240401. Available from: <https://link.aps.org/doi/10.1103/PhysRevLett.111.240401>.
- [29] Binder FC, Vinjanampathy S, Modi K, Goold J. Quantacell: powerful charging of quantum batteries. *New Journal of Physics*. 2015 jul;17(7):075015. Available from: <https://doi.org/10.1088/1367-2630/17/7/075015>.
- [30] Campaioli F, Pollock FA, Binder FC, Céleri L, Goold J, Vinjanampathy S, et al. Enhancing the Charging Power of Quantum Batteries. *Phys Rev Lett*. 2017 Apr;118:150601. Available from: <https://link.aps.org/doi/10.1103/PhysRevLett.118.150601>.
- [31] Le TP, Levinsen J, Modi K, Parish MM, Pollock FA. Spin-chain model of a many-body quantum battery. *Phys Rev A*. 2018 Feb;97:022106. Available from: <https://link.aps.org/doi/10.1103/PhysRevA.97.022106>.
- [32] Ferraro D, Campisi M, Andolina GM, Pellegrini V, Polini M. High-Power Collective Charging of a Solid-State Quantum Battery. *Physical Review Letters*. 2018 mar;120(11). Available from: <https://doi.org/10.1103/PhysRevLett.120.117702>.
- [33] Caravelli F, Coulter-De Wit G, García-Pintos LP, Hama A. Random quantum batteries. *Phys Rev Research*. 2020 Apr;2:023095. Available from: <https://link.aps.org/doi/10.1103/PhysRevResearch.2.023095>.
- [34] Zhao F, Dou FQ, Zhao Q. Charging performance of the Su-Schrieffer-Heeger quantum battery. *Phys Rev Research*. 2022 Mar;4:013172. Available from: <https://link.aps.org/doi/10.1103/PhysRevResearch.4.013172>.
- [35] Allahverdyan AE, Balian R, Nieuwenhuizen TM. Maximal work extraction from finite quantum systems. *Europhysics Letters (EPL)*. 2004 aug;67(4):565–571. Available from: <https://doi.org/10.1209/epl/i2004-10101-2>.
- [36] Santos AC, Çakmak Bieifmc, Campbell S, Zinner NT. Stable adiabatic quantum batteries. *Phys Rev E*. 2019 Sep;100:032107. Available from: <https://link.aps.org/doi/10.1103/PhysRevE.100.032107>.
- [37] Quach JQ, Munro WJ. Using Dark States to Charge and Stabilize Open Quantum Batteries. *Phys Rev Applied*. 2020 Aug;14:024092. Available from: <https://link.aps.org/doi/10.1103/PhysRevApplied.14.024092>.
- [38] Gherardini S, Campaioli F, Caruso F, Binder FC. Stabilizing open quantum batteries by sequential measurements. *Phys Rev Research*. 2020 Jan;2:013095. Available from: <https://link.aps.org/doi/10.1103/PhysRevResearch.2.013095>.
- [39] Mitchison MT, Goold J, Prior J. Charging a quantum battery with linear feedback control. *Quantum*. 2021 jul;5:500. Available from: <https://doi.org/10.22331/qf-2021-07-13-500>.
- [40] Zhu W, Rabitz H. A rapid monotonically convergent iteration algorithm for quantum optimal control over the expectation value of a positive definite operator. *The Journal of Chemical Physics*. 1998;109(2):385–391. Available from: <https://doi.org/10.1063/1.476575>.
- [41] Werschnik J, Gross EKU. Quantum optimal control theory. *Journal of Physics B: Atomic, Molecular and Optical Physics*. 2007 sep;40(18):R175–R211. Available from: <https://doi.org/10.1088/0953-4075/40/18/r01>.
- [42] Goerz M, Basilewitsch D, Gago-Encinas F, Krauss MG, Horn KP, Reich DM, et al. Krotov: A Python implementation of Krotov's method for quantum optimal control. *SciPost Physics*. 2019 dec;7(6). Available from: <https://doi.org/10.21468/SciPostPhys.7.6.080>.
- [43] Farina D, Andolina GM, Mari A, Polini M, Giovannetti V. Charger-mediated energy transfer for quantum batteries: An open-system approach. *Physical Review B*. 2019;99(3):035421.
- [44] Chruściński D, Pascazio S. A brief history of the GKLS equation. arXiv preprint arXiv:171005993. 2017.
- [45] Ferraro D, Campisi M, Andolina GM, Pellegrini V, Polini M. High-power collective charging of a solid-state quantum battery. *Physical review letters*. 2018;120(11):117702.
- [46] Andolina GM, Keck M, Mari A, Giovannetti V, Polini M. Quantum versus classical many-body batteries. *Physical Review B*. 2019;99(20):205437.
- [47] Julià-Farré S, Salamon T, Riera A, Bera MN, Lewenstein M. Bounds on the capacity and power of quantum

- batteries. *Physical Review Research*. 2020;2(2):023113.
- [48] Serafini A. *Quantum Continuous Variables: A Primer of Theoretical Methods*. Boca Raton, FL: CRC Press; 2017.
- [49] Blais A, Grimsmo AL, Girvin SM, Wallraff A. Circuit quantum electrodynamics. *Rev Mod Phys*. 2021 May;93:025005. Available from: <https://link.aps.org/doi/10.1103/RevModPhys.93.025005>.
- [50] Arute F, Arya K, Babbush R, Bacon D, Bardin JC, Barends R, et al. Quantum supremacy using a programmable superconducting processor. *Nature*. 2019 Oct;574(7779):505–510. Available from: <https://doi.org/10.1038/s41586-019-1666-5>.
- [51] Raftery J, Sadri D, Schmidt S, Türeci HE, Houck AA. Observation of a Dissipation-Induced Classical to Quantum Transition. *Phys Rev X*. 2014 Sep;4:031043. Available from: <https://link.aps.org/doi/10.1103/PhysRevX.4.031043>.
- [52] Wulschner F, Goetz J, Koessel FR, Hoffmann E, Baust A, Eder P, et al. Tunable coupling of transmission-line microwave resonators mediated by an rf SQUID. *EPJ Quantum Technology*. 2016 Jul;3(1):10. Available from: <https://doi.org/10.1140/epjqt/s40507-016-0048-2>.
- [53] Miyanaga T, Tomonaga A, Ito H, Mukai H, Tsai JS. Ultrastrong Tunable Coupler Between Superconducting LC Resonators. *Phys Rev Applied*. 2021 Dec;16:064041. Available from: <https://link.aps.org/doi/10.1103/PhysRevApplied.16.064041>.
- [54] Bockstiegel C, Wang Y, Vissers MR, Wei LF, Chaudhuri S, Hubmayr J, et al. A tunable coupler for superconducting microwave resonators using a nonlinear kinetic inductance transmission line. *Applied Physics Letters*. 2016;108(22):222604. Available from: <https://doi.org/10.1063/1.4953209>.
- [55] Chow JM, DiCarlo L, Gambetta JM, Motzoi F, Frunzio L, Girvin SM, et al. Optimized driving of superconducting artificial atoms for improved single-qubit gates. *Phys Rev A*. 2010 Oct;82:040305. Available from: <https://link.aps.org/doi/10.1103/PhysRevA.82.040305>.
- [56] Li K, McDermott R, Vavilov MG. Hardware-Efficient Qubit Control with Single-Flux-Quantum Pulse Sequences. *Phys Rev Applied*. 2019 Jul;12:014044. Available from: <https://link.aps.org/doi/10.1103/PhysRevApplied.12.014044>.
- [57] Egger DJ, Wilhelm FK. Adaptive Hybrid Optimal Quantum Control for Imprecisely Characterized Systems. *Phys Rev Lett*. 2014 Jun;112:240503. Available from: <https://link.aps.org/doi/10.1103/PhysRevLett.112.240503>.
- [58] Werninghaus M, Egger DJ, Roy F, Machnes S, Wilhelm FK, Filipp S. Leakage reduction in fast superconducting qubit gates via optimal control. *npj Quantum Information*. 2021 Jan;7(1):14. Available from: <https://doi.org/10.1038/s41534-020-00346-2>.
- [59] Gerry C, Knight P, Knight PL. *Introductory quantum optics*. Cambridge university press; 2005.
- [60] Reich DM, Ndong M, Koch CP. Monotonically convergent optimization in quantum control using Krotov’s method. *The Journal of Chemical Physics*. 2012 Mar;136(10):104103. Available from: <https://aip.scitation.org/doi/10.1063/1.3691827>.
- [61] Koch CP. Controlling open quantum systems: tools, achievements, and limitations. *Journal of Physics: Condensed Matter*. 2016 Jun;28(21):213001. Available from: <https://iopscience.iop.org/article/10.1088/0953-8984/28/21/213001>.
- [62] In general though, $\hat{\sigma}_k^{(i-1)}(T) = -\frac{\partial J_T}{\partial \hat{\rho}_k(T)} \Big|_{(i-1)}$. For the cases computed in the paper, equation 9 is enough.
- [63] As the second moments matrix V is symmetric, we will just use the elements of the upper triangular part of the matrix.